

# Neural Network-Based Modeling and Parameter Identification of Switched Reluctance Motors

Wenzhe Lu, *Student Member, IEEE*, Ali Keyhani, *Fellow, IEEE*, and Abbas Fardoun, *Member, IEEE*

**Abstract**—Phase windings of switched reluctance machines are modeled by a nonlinear inductance and a resistance that can be estimated from standstill test data. During online operation, the model structures and parameters of SRMs may differ from the standstill ones because of saturation and losses, especially at high current. To model this effect, a damper winding is added into the model structure. This paper proposes an application of artificial neural network to identify the nonlinear model of SRMs from operating data. A two-layer recurrent neural network has been adopted here to estimate the damper currents from phase voltage, phase current, rotor position, and rotor speed. Then, the damper parameters can be identified using maximum likelihood estimation techniques. Finally, the new model and parameters are validated from operating data.

**Index Terms**—Modeling, neural network, parameter identification, switched reluctance motor.

## I. INTRODUCTION

SWITCHED reluctance motors (SRMs) have undergone rapid development in hybrid electric vehicles, aircraft starter/generator systems, washing machines, and automotive applications over the last two decades. This is mainly due to the various advantages of SRMs over other electric motors such as simple and robust construction, and fault-tolerant performance.

In most of these applications, speed and torque control are necessary. To obtain high quality control, an accurate model of the SRM is often needed. At the same time, to increase reliability and reduce cost, sensorless controllers (without rotor position/speed sensor) are preferred. With the rapid progress in microprocessors (DSP), MIPS-intensive control techniques such as sliding mode observers and controllers [1] become more and more promising. An accurate nonlinear model of the SRM is essential to realize such control algorithms.

The nonlinear nature of SRM and high saturation of phase winding during operation makes the modeling of SRM a challenging work. The flux linkage and phase inductance of SRM change with both the rotor position and the phase current. Therefore, the nonlinear model of SRM must be identified as a function of the phase current and rotor position. Two main models of SRM have been suggested in the literature—the flux model [2] and the inductance model [3]. In the latter one, “the position dependency of the phase inductance is represented by a limited number of Fourier series terms and the nonlinear variation of

the inductance with current is expressed by means of polynomial functions” [3]. This model can describe the nonlinearity of SRM inductance quite well.

Once a model is selected, how to identify the parameters in the model becomes an important issue. Finite element analysis can provide a model that will be subjected to substantial variation after the machine is constructed with manufacturing tolerances. Therefore, the model and parameters need to be identified from test data. As a first step, the machine model can be estimated from standstill test using maximum likelihood estimation (MLE) techniques. This method has already been applied successfully to identify the model and parameters of induction and synchronous machines [4], [5].

Furthermore, during online operation, the model structures and parameters of SRMs may differ from the standstill ones because of saturation and losses, especially at high current. To model this effect, a damper winding may be added into the model structure, which is in parallel with the magnetizing winding. The magnetizing current and damper current are highly nonlinear functions of phase voltage, rotor position, and rotor speed. They are not measurable during operation, and are hard to be expressed with analytical functions. Neural network mapping are usually good choices for such tasks [7]–[9]. A two-layer recurrent neural network has been adopted here to estimate these two currents, which takes the phase voltage, phase current, rotor position, and rotor speed as inputs. When the damper current is estimated and damper voltage is computed, the damper parameters can be identified using output error or maximum likelihood estimation techniques.

In this paper, the procedures to identify an 8/6 SRM parameters from standstill test data are presented after a brief introduction to the inductance model of SRM. Then a two-layer recurrent neural network is trained and applied to identify the damper parameters of SRM from operating data. Model validation through online test is also given, which proves the applicability of the proposed methods.

## II. INDUCTANCE MODEL OF SRM AT STANDSTILL

The inductance model of switched reluctance motor is shown in Fig. 1.

Since the phase inductance changes periodically with the rotor position angle, it can be expressed as a Fourier series with respect to rotor position angle  $\theta$

$$L(\theta, i) = \sum_{k=0}^m L_k(i) \cos kN_r\theta \quad (1)$$

where  $N_r$  is the number of rotor poles.

To determine the coefficients  $L_k(i)$  in the Fourier series, we need to know the inductances at several specific positions. Use

Manuscript received July 25, 2002. This work is supported in part by NSF Grant ECS0105320, and in part by TRW and Delphi Automotive Systems.

W. Lu and A. Keyhani are with the Department of Electrical Engineering, The Ohio State University, Columbus, OH 43210 (e-mail: keyhani.1@osu.edu).

A. Fardoun is with TRW Automotive, Sterling Heights, MI 48311 (e-mail: abbas.fardoun@trw.com).

Digital Object Identifier 10.1109/TEC.2003.811738

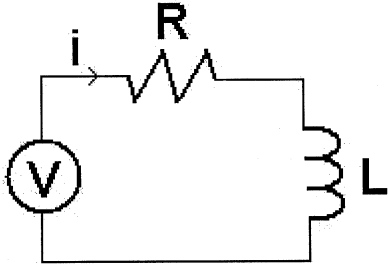


Fig. 1. Inductance model of SRM at standstill.

$L_\theta(i)$  to represent the inductance at position  $\theta$ , which is a function of phase current  $i$  and can be approximated by a polynomial

$$L_\theta(i) = \sum_{n=0}^p a_{\theta,n} i^n \quad (2)$$

where  $p$  is the order of the polynomial and  $a_{\theta,n}$  are the coefficients of polynomial. In our research,  $p = 5$  is chosen after we compare the fitting results of different  $p$  values (we tried  $p = 3, 4, 5$ , and  $6$ ).

For an 8/6 machine,  $N_r = 6$ . When  $\theta = 0^\circ$  is chosen at the aligned position of phase A, then  $\theta = 30^\circ$  is the unaligned position of phase A. Usually, the inductance at unaligned can be treated as a constant [3]:

$$L_{30^\circ} = \text{const.} \quad (3)$$

In [3], the authors suggest using the first three terms of the Fourier series, but more terms can be added to meet accuracy requirements.

#### A. Three-Term Inductance Model

If three terms are used in the Fourier series, then we can compute the three coefficients  $L_0$ ,  $L_1$ , and  $L_2$  from  $L_{0^\circ}$  (aligned position),  $L_{30^\circ}$  (unaligned position), and  $L_{15^\circ}$  (a midway between the above two positions). Since

$$\begin{bmatrix} L_{0^\circ} \\ L_{15^\circ} \\ L_{30^\circ} \end{bmatrix} = \begin{bmatrix} 1 & 1 & 1 \\ 1 & \cos(6 * 15^\circ) & \cos(12 * 15^\circ) \\ 1 & \cos(6 * 30^\circ) & \cos(12 * 30^\circ) \end{bmatrix} \begin{bmatrix} L_0 \\ L_1 \\ L_2 \end{bmatrix}, \quad (4)$$

we have

$$\begin{bmatrix} L_0 \\ L_1 \\ L_2 \end{bmatrix} = \begin{bmatrix} \frac{1}{4} & \frac{1}{2} & \frac{1}{4} \\ \frac{1}{2} & 0 & -\frac{1}{2} \\ \frac{1}{4} & -\frac{1}{2} & \frac{1}{4} \end{bmatrix} \begin{bmatrix} L_{0^\circ} \\ L_{15^\circ} \\ L_{30^\circ} \end{bmatrix}. \quad (5)$$

#### B. Four-Term Inductance Model

If four terms are used in the Fourier series, then we can compute the four coefficients  $L_0$ ,  $L_1$ ,  $L_2$ , and  $L_3$  from  $L_{0^\circ}$  (aligned position),  $L_{10^\circ}$ ,  $L_{20^\circ}$ , and  $L_{30^\circ}$  (unaligned position). Since

$$\begin{bmatrix} L_{0^\circ} \\ L_{10^\circ} \\ L_{20^\circ} \\ L_{30^\circ} \end{bmatrix} = \begin{bmatrix} 1 & 1 & 1 & 1 \\ 1 & \cos(60^\circ) & \cos(120^\circ) & \cos(180^\circ) \\ 1 & \cos(120^\circ) & \cos(240^\circ) & \cos(360^\circ) \\ 1 & \cos(180^\circ) & \cos(360^\circ) & \cos(540^\circ) \end{bmatrix} \times \begin{bmatrix} L_0 \\ L_1 \\ L_2 \\ L_3 \end{bmatrix} \quad (6)$$

we have

$$\begin{bmatrix} L_0 \\ L_1 \\ L_2 \\ L_3 \end{bmatrix} = \begin{bmatrix} \frac{1}{6} & \frac{1}{3} & \frac{1}{3} & \frac{1}{6} \\ \frac{1}{3} & \frac{1}{3} & -\frac{1}{3} & -\frac{1}{3} \\ \frac{1}{3} & -\frac{1}{3} & -\frac{1}{3} & \frac{1}{3} \\ \frac{1}{6} & -\frac{1}{3} & \frac{1}{3} & -\frac{1}{6} \end{bmatrix} \begin{bmatrix} L_{0^\circ} \\ L_{10^\circ} \\ L_{20^\circ} \\ L_{30^\circ} \end{bmatrix}. \quad (7)$$

#### C. Voltage Equation and Torque Computation

Based on the inductance model described before, the phase voltage equations can be formed and the electromagnetic torque can be computed from the partial derivative of magnetic co-energy with respect to rotor angle  $\theta$ . They are listed here

$$\begin{aligned} V &= R \cdot i + \frac{d\psi}{dt} = R \cdot i + \frac{d(Li)}{dt} \\ &= R \cdot i + L \frac{di}{dt} + i \left( \frac{\partial L}{\partial \theta} \omega + \frac{\partial L}{\partial i} \frac{di}{dt} \right) \end{aligned} \quad (8)$$

where

$$\begin{aligned} \omega &= \frac{d\theta}{dt} \\ \frac{\partial L}{\partial i} &= \sum_{k=0}^m \frac{\partial L_k(i)}{\partial i} \cos k N_r \theta \end{aligned} \quad (9)$$

$$\frac{\partial L}{\partial \theta} = - \sum_{k=1}^m L_k(i) k N_r \sin k N_r \theta. \quad (10)$$

And

$$\begin{aligned} T &= \frac{\partial W_c(\theta, i)}{\partial \theta} = \frac{\partial \left\{ \int [L(\theta, i) i] di \right\}}{\partial \theta} \\ &= \frac{\partial \left\{ \int \sum_{k=0}^m [L_k(i) \cos(k N_r \theta) i] di \right\}}{\partial \theta} \\ &= - \sum_{k=1}^m \left\{ k N_r \sin(k N_r \theta) \int [L_k(i) i] di \right\}. \end{aligned} \quad (11)$$

### III. MAXIMUM LIKELIHOOD ESTIMATION

To minimize the effects of noise caused by the converter harmonics and the measurement, maximum likelihood estimation (MLE) technique can be applied to estimate the parameters. Suppose the dynamic response of the system is represented by

$$\begin{cases} x(k+1) = A(\theta_p)x(k) + B(\theta_p)u(k) + w(k) \\ y(k) = C(\theta_p)x(k) + v(k), \end{cases} \quad (12)$$

where  $\theta_p$  represents the system parameters,  $x(k)$  represents system states,  $y(k)$  represents the system output,  $u(k)$  is the system input,  $w(k)$  is the process noise, and  $v(k)$  is the measurement noise.

The maximum likelihood estimation is performed based on the mechanism shown in Fig. 2. A model of the phase winding is excited with the same voltage as the real winding. The error between the estimated output and the measured output is used to adjust the model parameters (according to output error estimation algorithm) to minimize the cost function  $V(\theta)$ . This process is repeated till the cost function is minimized.

The model structure in Fig. 1 is a first-order system. The dynamic equation for it can be expressed as

$$V = R \cdot i + L \frac{di}{dt}. \quad (13)$$

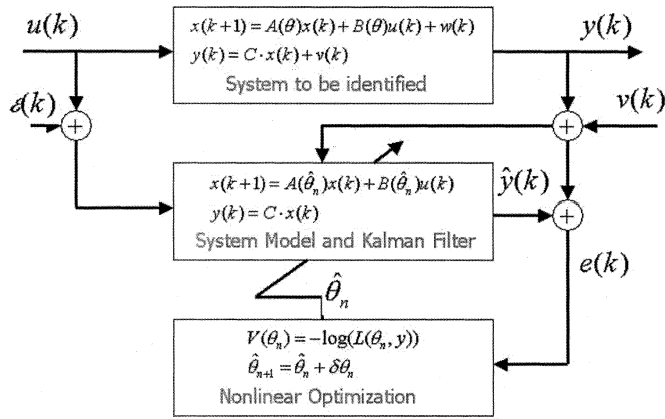


Fig. 2. Block diagram of maximum likelihood estimation.

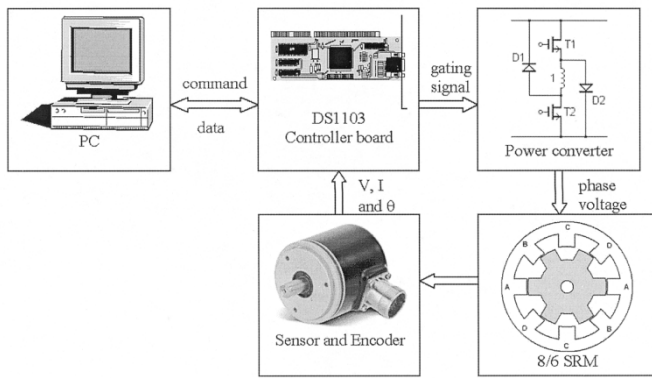


Fig. 3. Experimental setup.

When transformed to discrete-time state space form, the states, input, output, and parameters vector are

$$\begin{aligned} x &= [i], & u &= [V], & y &= [i] \\ \theta_p &= [R, L]^T. \end{aligned} \quad (14)$$

#### IV. PARAMETER IDENTIFICATION FROM STANDSTILL TEST DATA

The basic idea of standstill test is to apply a short voltage pulse to the phase winding with the rotor blocked, record the current generated in the winding, and then use maximum likelihood estimation to estimate the resistances and inductances of the winding. By performing this test at a different current level, the relationship between inductance and current can be curve-fitted with polynomials.

The experimental setup is shown in Fig. 3. An 8/6 SRM is used in this test. Before testing, the motor is rotated to a specific position (with one of the phase windings aligned, unaligned, or at other positions) and blocked. A DSP system (dSPACE DS1103 controller board) is used to generate the gating signal to a power converter to apply appropriate voltage pulses to that winding. The voltage and current at the winding is sampled and recorded. Later on, the test data are used to identify the winding parameters.

The motor used in this test is an 8/6 SRM. Tests are performed at several specific positions for current between 0–50 A. The

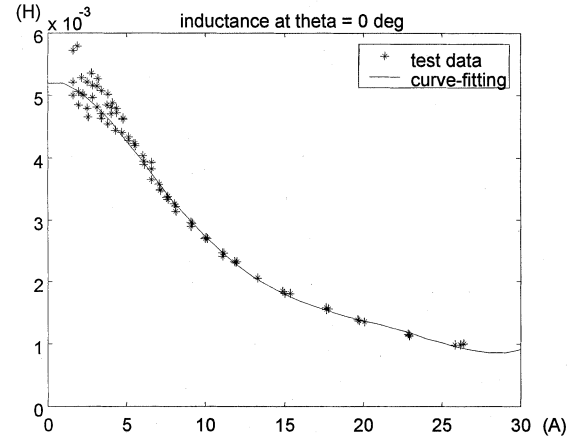


Fig. 4. Standstill test results for inductance at 0°.

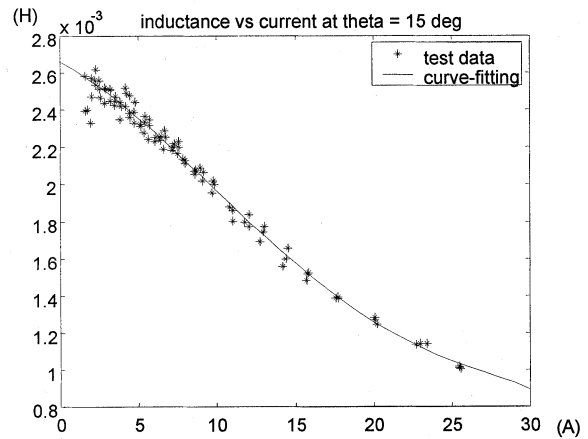


Fig. 5. Standstill test results for inductance at 15°.

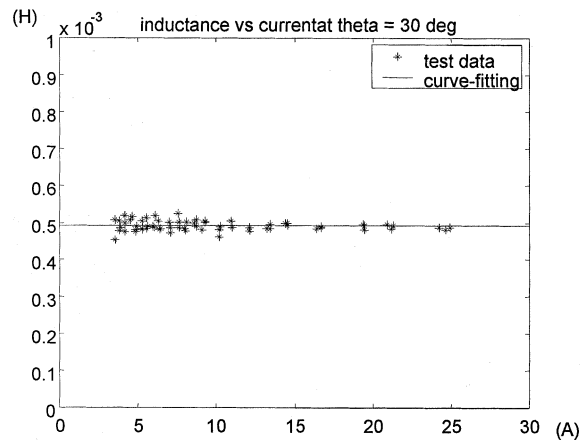


Fig. 6. Standstill test results for inductance at 30°.

inductance estimation and curve-fitting results at aligned, midway, and unaligned position are shown in Fig. 4–6 (Results are obtained using Matlab/Simulink®).

The results show that the inductance at unaligned position does not change much with the phase current and can be treated as a constant. The inductances at midway and aligned position

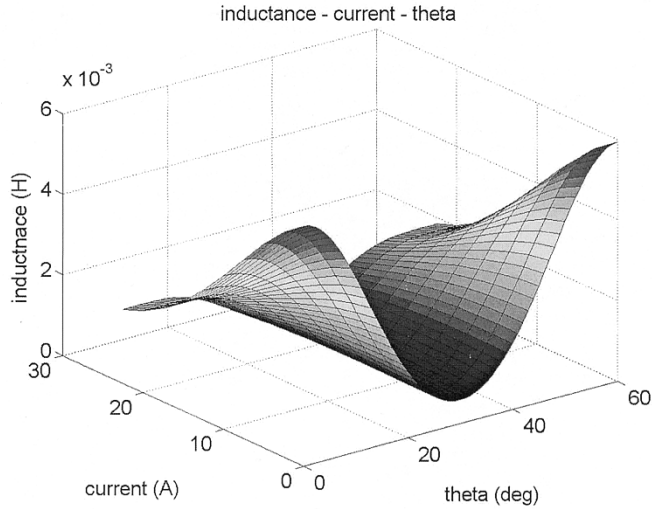


Fig. 7. Standstill test result: nonlinear phase inductance.

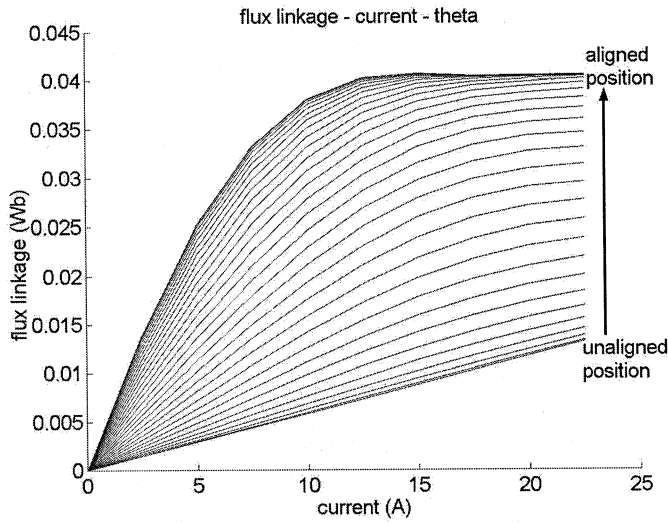


Fig. 8. Flux linkage at different currents and different rotor positions.

decrease when current increases due to saturation. A three-dimensional (3-D) plot of inductance shown in Fig. 7 depicts the profile of inductance versus rotor position and phase current.

At  $\theta = 0$  and  $60^\circ$ , phase A is at its aligned positions and has the highest value of inductance. It decreases when the phase current increases. At  $\theta = 30^\circ$ , phase A is at its unaligned position and has lowest value of inductance. The inductance here keeps nearly constant when the phase current changes.

In Fig. 8, the flux linkage versus rotor position and phase current based on the estimated inductance model is shown. The saturation of phase winding at high currents is clearly represented. At aligned position, the winding is highly saturated at rated current.

## V. SRM MODEL FOR ONLINE OPERATION

For online operation case, especially under high load, the losses become significant. There are no windings on the rotor of SRMs. But similar as synchronous machines, there will be circulating currents flowing in the rotor body and makes it work as

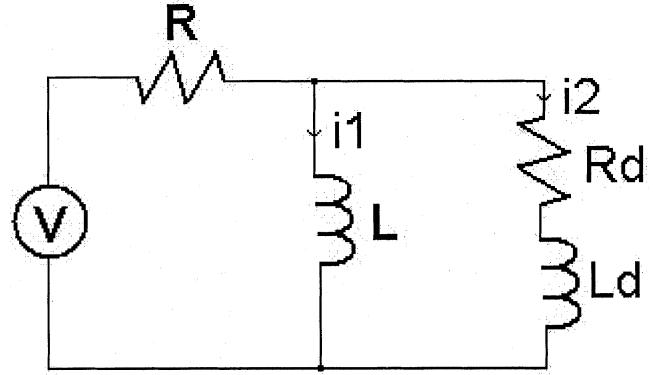


Fig. 9. Model structure of SRM under saturation.

a damper winding. Considering this, the model structure may be modified as shown in Fig. 9, with  $R_d$  and  $L_d$  added to represent the losses on the rotor.

The phase voltage equations can be written as

$$\begin{bmatrix} L & -L_d \\ 0 & L_d \end{bmatrix} \cdot \begin{bmatrix} \dot{i}_1 \\ \dot{i}_2 \end{bmatrix} = \begin{bmatrix} 0 & R_d \\ -R & -R - R_d \end{bmatrix} \cdot \begin{bmatrix} i_1 \\ i_2 \end{bmatrix} + \begin{bmatrix} 0 \\ 1 \end{bmatrix} V \quad (15)$$

where  $i_1$  and  $i_2$  are the magnetizing current and damper current.

It can be rewritten in state space form as

$$\begin{aligned} \dot{X} &= AX + BU \\ Y &= CX + DU \end{aligned} \quad (16)$$

where

$$\begin{aligned} X &= [i_1 \quad i_2], \quad Y = i_1 + i_2, \quad U = [V] \\ A &= \begin{bmatrix} L & -L_d \\ 0 & L_d \end{bmatrix}^{-1} \cdot \begin{bmatrix} 0 & R_d \\ -R & -R - R_d \end{bmatrix}, \\ B &= \begin{bmatrix} L & -L_d \\ 0 & L_d \end{bmatrix}^{-1} \cdot \begin{bmatrix} 0 \\ 1 \end{bmatrix}, \\ C &= [1 \quad 1], \text{ and} \\ D &= 0. \end{aligned}$$

The torque can be computed as follows (notice that  $L$  is the magnetizing winding):

$$\begin{aligned} T &= \frac{\partial W_c(\theta, i_1)}{\partial \theta} = \frac{\partial \left\{ \int [L(\theta, i_1) i_1] di_1 \right\}}{\partial \theta} \\ &= \frac{\partial \left\{ \int \sum_{k=0}^m [L_k(i_1) \cos(kN_r \theta)] i_1 di_1 \right\}}{\partial \theta} \\ &= - \sum_{k=1}^m \left\{ kN_r \sin(kN_r \theta) \int [L_k(i_1) i_1] di_1 \right\}. \end{aligned} \quad (17)$$

During operation, we can easily measure phase voltage  $V$  and phase current  $i = i_1 + i_2$ . But we cannot measure the magnetizing current ( $i_1$ ) and the damper winding current ( $i_2$ ). Let's assume that the phase parameters  $R$  and  $L$  obtained from standstill test data are accurate enough for low current case. And we want to attribute all of the errors at high current case to damper parameters. If we can estimate the exciting  $i_1$  during online operation, then it will be very easy to estimate the damper parameters. This is described in Sections VI–IX.

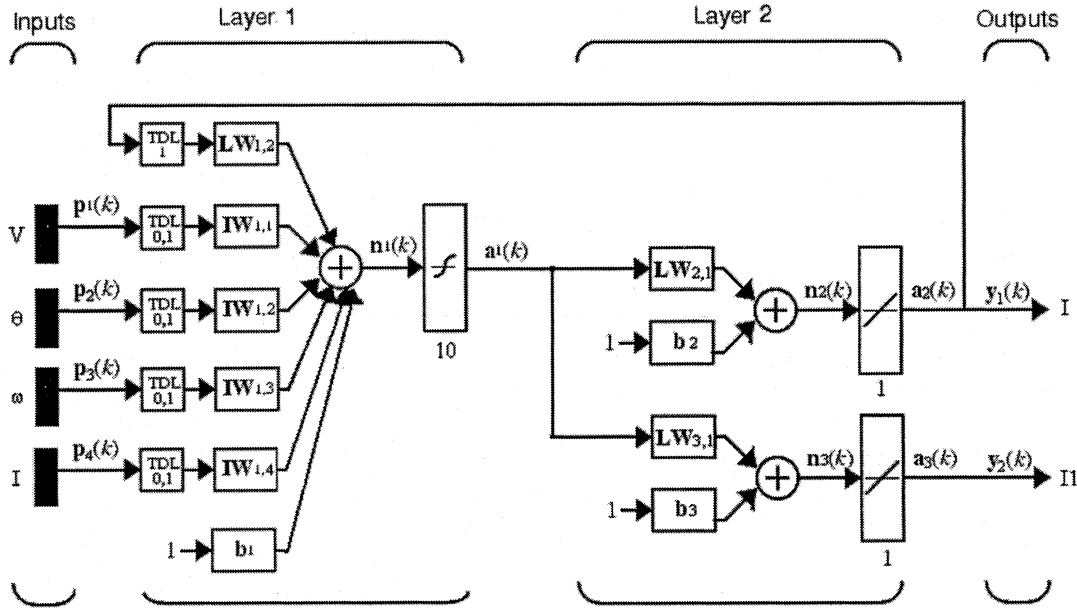


Fig. 10. Recurrent neural network structure for estimation of exciting current.

## VI. TWO-LAYER RECURRENT NEURAL NETWORK

During online operation, there will be motional back EMF in the phase winding. So the exciting current  $i_1$  will be affected by

- phase voltage  $V$ ;
- phase current  $i$ ;
- rotor position  $\theta$ ;
- rotor speed  $\omega$ .

To map the relationship between  $i_1$  and  $V$ ,  $i$ ,  $\theta$ ,  $\omega$ , different neural network structures (feed forward or recurrent), with different number of layers, different number of neurons in each layer, and different transfer functions for each neuron, are tried. Finally the one shown in Fig. 10 is used. It is a two-layer recurrent neural network. The feeding-back of the output  $i$  to input makes it better in fitting and faster in convergence.

The first layer is the input layer. The inputs of the network are  $V$ ,  $i$ ,  $\theta$ , and  $\omega$  (with possible delays). One of the outputs, the current  $i$  is also fed back to the input layer to form a recurrent neural network.

The second layer is the output layer. The outputs are  $i$  (used as training objective) and  $\hat{i}_1$ .

A hyperbolic tangent sigmoid transfer function—"tansig()" is chosen to be the activation function of the input layer, which gives the following relationship between its inputs and outputs:

$$n_1 = \sum_{i=1}^4 IW_{1,i} \cdot p_i + LW_{1,2} \cdot y_1 + b_1$$

$$a_1 = \text{tansig}(n_1) = \frac{2}{1 + e^{-2n_1}} - 1. \quad (18)$$

A pure linear function is chosen to be the activation of the output layers, which gives

$$n_2 = LW_{2,1} \cdot a_1 + b_2$$

$$y_1 = a_2 = \text{purelin}(n_2) = n_2; \quad (19)$$

$$n_3 = LW_{3,1} \cdot a_1 + b_3$$

$$y_2 = a_3 = \text{purelin}(n_3) = n_3. \quad (20)$$

After the neural network is trained with simulation data (using parameters obtained from standstill test). It can be used to estimate exciting current during online operation. When  $\hat{i}_1$  is estimated, the damper current can be computed as

$$i_2 = i - \hat{i}_1 \quad (21)$$

and the damper voltage can be computed as

$$V_2 = V - i \cdot R \quad (22)$$

then the damper resistance  $R_d$  and inductance  $L_d$  can be identified using output error or maximum likelihood estimation.

## VII. TRAINING OF NEURAL NETWORK

The data used for training are generated from simulation of SRM model obtained from standstill test. The model is simulated at different dc voltages, different reference currents, and different speed. The total size of the sample data is 13 351 800 data points. The training procedure is detailed as follows:

First, from standstill test result, we can estimate the winding parameters ( $R$  and  $L$ ) and damper parameters ( $R_d$  and  $L_d$ ). The  $R_d$  and  $L_d$  got from standstill test data may not be accurate enough for online model, but it can be used as initial values that will be improved later.

Second, build an SRM model with above parameters and simulate the motor with hysteresis current control and speed control. The operating data under different reference currents and different rotor speeds are collected and sent to neural network for training.

Third, when training is done, use the trained ANN model to estimate the magnetizing current ( $\hat{i}_1$ ) from online operating data. Compute damper voltage and current according to (21) and (22). Then, estimate  $R_d$  and  $L_d$  from the computed  $V_2$  and  $i_2$  using output error estimation. This  $R_d$  and  $L_d$  can be treated as improved values of standstill test results.

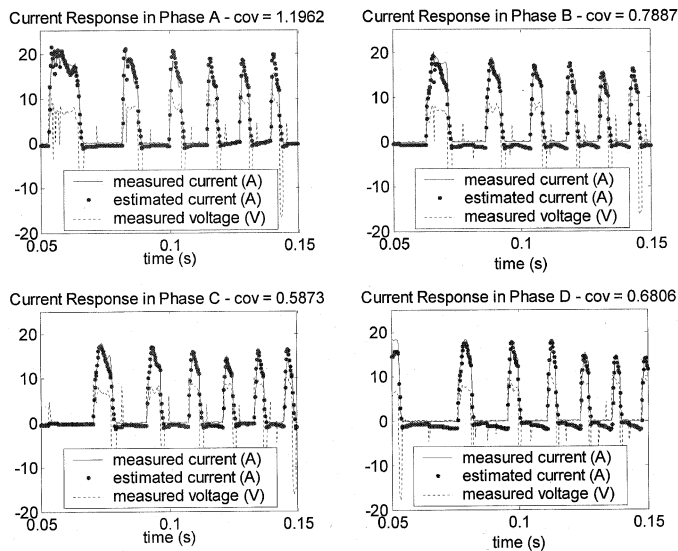


Fig. 11. Validation of model with online operating data.

Repeat above procedures until  $R_d$  and  $L_d$  are accurate enough to represent online operation (it means that the simulation data matches the measurements well).

In our research, the neural network can map the exciting current from  $V$ ,  $i$ ,  $\theta$ ,  $\omega$  very well after training of 200 epochs.

### VIII. ESTIMATION RESULTS

The parameters for damper winding are successfully estimated from operating data by using the neural network mapping described before.

To test the validity of the parameters obtained from above test, a simple online test has been performed. In this test, the motor is accelerated with a fixed reference current of 20 A. All of the operating data such as phase voltages, currents, rotor position, and rotor speed are measured. Then, the phase voltages are fed to an SRM model running in Simulink, which has the same rotor position and speed as the real motor. All of the phase currents are estimated from the Simulink mode and compared with the measured currents. In Fig. 11, the phase current responses are shown. The dashed curve is the voltage applied to phase winding; the solid curve is the measured current; and the dotted curve is the estimated current. An enlarged view of the curves for phase A is shown in Fig. 12. It is clear that the estimation approximates to the measurement quite well.

To compare online model with standstill one, we compute the covariance of the errors between the estimated phase currents and the measured currents. The average covariance for standstill model is 0.9127, while that for online model is 0.6885. It means that the online model gives much better estimation of operating phase currents.

### IX. ADVANTAGES OF USING NEURAL NETWORK MAPPING

During online operation, the exciting current  $i_1$  changes with phase voltage  $V$ , rotor position  $\theta$ , and rotor speed  $\omega$ . The relationship between them is highly nonlinear and cannot be easily expressed by any analytical equation. The neural network can

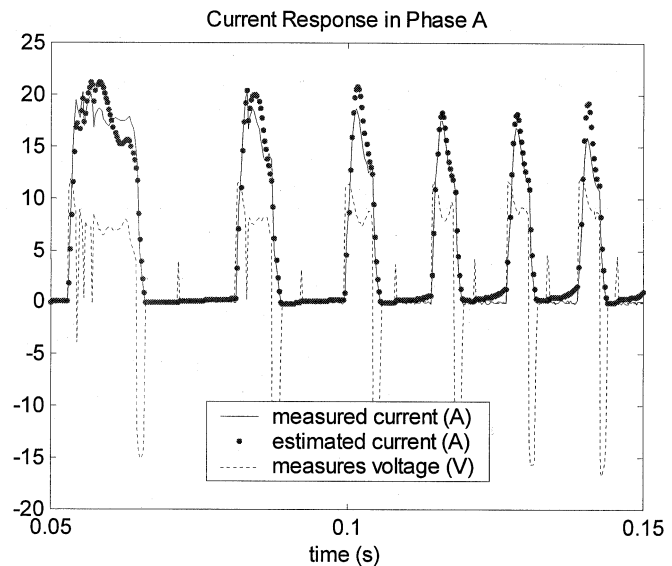


Fig. 12. Validation of model with online operating data (phase A).

provide very good mapping if trained correctly. This makes it a good choice for such a task.

Once the NN is trained, it can estimate the exciting current from inputs very quickly, without solving any differential equations that is necessary in conventional methods. So it can be used for online parameter identification with no computational difficulties. This method has been successfully applied to synchronous machines and induction machines [6], [8], [9]; it can be applied to SRMs as well.

### X. CONCLUSIONS

This paper presents the idea and procedure to use artificial neural network to help identify the resistance and nonlinear inductance of SRM winding from operating data. First, the resistance and inductance of the magnetizing winding are identified from standstill test data. Then, a two-layer recurrent neural network is setup and trained with simulation data based on standstill model. By applying this neural network to online operating data, the magnetizing current can be estimated and the damper current can be computed. Then, the parameters of the damper winding can be identified using maximum likelihood estimation. Tests performed on a 50-A 8/6 SRM show satisfactory results of this method.

### REFERENCES

- [1] V. Utkin, J. Guldner, and J. Shi, *Sliding Model Control in Electro-mechanical Systems*. New York: Taylor & Francis, 1999.
- [2] S. Mir, I. Husain, and M. E. Elbuluk, "Switched reluctance motor modeling with on-line parameter identification," *IEEE Trans. Ind. Applicat.*, vol. 34, pp. 776–783, July/Aug. 1998.
- [3] B. Fahimi, G. Suresh, J. Mahdavi, and M. Ehsani, "A new approach to model switched reluctance motor drive application to dynamic performance prediction, control and design," in *Power Electron. Specialists Conf.*, vol. 2, 1998.
- [4] L. Xu and E. Ruckstadter, "Direct modeling of switched reluctance machine by coupled field-circuit method," *IEEE Trans. Energy Conversion*, vol. 10, pp. 446–454, Sept. 1995.
- [5] S.-I. Moon and A. Keyhani, "Estimation of induction machine parameters from standstill time-domain data," *IEEE Trans. Ind. Applicat.*, vol. 30, Nov./Dec. 1994.

- [6] A. Keyhani, H. Tsai, and T. Leksan, "Maximum likelihood estimation of synchronous machine parameters from standstill time response data," in *Proc. IEEE/Power Eng. Soc. Winter Meeting*, Columbus, OH, Jan./Feb. 31–5, 1993.
- [7] K. M. Passino, "Intelligent control: Biomimicry for optimization, adaptation, and decision-making in computer control and automation," in *EE858 Textbook*. Columbus, OH: The Ohio State Univ., 2001.
- [8] S. Pillutla and A. Keyhani, "Neural network based modeling of round rotor synchronous generator rotor body parameters from operating data," *IEEE Trans. Energy Conversion*, vol. 14, pp. 321–327, Sept. 1999.
- [9] —, "Neural network based saturation model of round rotor synchronous generator rotor," *IEEE Trans. Energy Conversion*, vol. 14, pp. 1019–1025, Dec. 1999.
- [10] S. S. Ramamurthy, R. M. Schupbach, and J. C. Balda, *Artificial Neural Networks based Models for the Multiply Excited Switched Reluctance Motor*: APEC, 2001.
- [11] B. Fahimi, G. Suresh, J. Mahdavi, and M. Ehsani, "A new approach to model switched reluctance motor drive application to dynamic performance prediction, control and design," in *Power Electron. Specialists Conf.*, vol. 2, 1998.

**Wenzhe Lu** (S'00) received the B.S. degree from Xi'an Jiaotong University, Xi'an, China, in 1993, and the M.S. degree from Tsinghua University, Beijing, China, in 1996. He is currently pursuing the Ph.D. degree in the Electrical Engineering Department at The Ohio State University, Columbus.

His research interests include modeling and control of switched reluctance motors for electric vehicle applications.

**Ali Keyhani** (S'72–M'76–SM'89–F'98) received the Ph.D. degree from Purdue University, West Lafayette, IN, in 1975.

Currently, he is a Professor of Electrical Engineering at the Ohio State University, Columbus, OH. From 1967 to 1969, he worked for Hewlett-Packard Co., Palo Alto, CA, on the computer-aided design of electronic transformers. From 1970 to 1973, he worked for Columbus and Southern Ohio Electric Co., Columbus, OH, on computer applications for power system engineering problems. In 1974, he joined TRW Controls, Houston, TX, and worked on the development of computer programs for energy control centers. From 1976 to 1980, he was a Professor of Electrical Engineering at Tehran Polytechnic, Tehran, Iran. His research interests are in control and modeling, parameter estimation, failure detection of electric machines, transformers, and drive systems.

**Abbas Fardoun** (M'90) was born in Tyre, Lebanon. He received the B.S. degree from the University of Houston, TX, in 1988, and the M.S. and Ph.D. degrees from the University of Colorado, Boulder, in 1990 and 1994, respectively.

Currently, he is with TRW Automotive, Sterling Heights, MI. He was with Advanced Energy, Inc., Fort Collins, CO, from 1994 to 1996 where he was involved with high frequency power supply design. From 1996 until 1998, he was with Delphi, Saginaw, MI, where he worked on Electrical Power Steering. He has several patents related to automotive applications. His main interests are ac drives, power electronics, and switched reluctance drives.

Dr. Fardoun received the Hariri Foundation distinguished graduate award in 1994 and he is the recipient of the TRW patent award in 1999.